# Transverse-Longitudinal Coupling Effect in Laser Bunch Slicing

M. Shimada,[1,*] M. Katoh,[2,3] M. Adachi,[2,3] T. Tanikawa,[3] S. Kimura,[2,3] M. Hosaka,[4] N. Yamamoto,[4] Y. Takashima,[4] and T. Takahashi[5]

[1]*High Energy Accelerator Research Organization, KEK, Tsukuba, 305-0801, Japan*
[2]*UVSOR, Institute for Molecular Science, Okazaki, 444-8585, Japan*
[3]*School of Physical Sciences, The Graduate University for Advanced Studies (SOKENDAI), Okazaki, 444-8585, Japan*
[4]*Graduate School for Engineering, Nagoya University, Nagoya, 464-8603, Japan*
[5]*Research Reactor Institute, Kyoto University, Kumatori-cho, 590-0494, Japan*

(Received 27 May 2009; published 1 October 2009)

We report turn-by-turn observation of coherent synchrotron radiation (CSR) produced by the laser bunch slicing technique at an electron storage ring operated with a small momentum compaction factor. CSR emission was intermittent, and its interval depended strongly on the betatron tune. This peculiar behavior of the CSR could be interpreted as a result of coupling between the transverse and longitudinal motion of the electrons. This is the first observation of such an effect, which would be important not only for controlling the CSR emission but also for generating and transporting ultrashort electron bunches or electron bunches with microdensity structures in advanced accelerators.

DOI: 10.1103/PhysRevLett.103.144802 PACS numbers: 41.60.Ap, 07.57.Hm, 29.27.Bd

Coherent synchrotron radiation (CSR) from relativistic electron bunches with lengths shorter than the radiation wavelength has been intensively investigated because of its potential ultrahigh power in the terahertz (THz) region [1]. THz CSR is expected to open a new aspect in the material, chemical, biological, and medical fields [2]. The first observation of CSR was achieved using 2.5 mm electron bunches produced by a linear accelerator [3]. Since then, CSR was produced exclusively by linear accelerators. However, in recent years, even on storage rings, THz CSR from submillimeter bunches was produced using an accelerator technique called low-alpha optics [4–6]. Construction of advanced circular accelerators dedicated to CSR production has been proposed [7–9].

CSR is emitted not only from short bunches but also from electron bunches with longitudinal microstructure of radiation wavelength scale. This is because CSR intensity is proportional to the square of the Fourier transform of the longitudinal density distribution of the electron bunch [10]. Laser bunch slicing is a technique for creating submillimeter dip structure on electron bunches using femtosecond laser pulses [11]. At several storage rings, intense and broadband THz CSR has been successfully produced by this technique [12–15]. In particular, at UVSOR-II (Japan), tunable and narrow band THz CSR has been successfully produced using amplitude-modulated laser pulses [16].

To effectively produce the THz CSR, the temporal evolution of longitudinal density structure is highly important. Usually in electron accelerators, long-term maintenance of longitudinal microstructures is difficult because they are easily destroyed by longitudinal slippage, in which the energy spread of the electrons turns to the spread of the longitudinal position. It is well known that this effect can be suppressed by adopting isochronous or low-alpha optics [17]. However, it was also explained theoretically that, after introducing such techniques, the transverse-longitudinal coupling effect becomes significant, in which transverse emittance turns into the spread of the longitudinal position and destroys longitudinal microstructures [18,19]. However, to our knowledge, no direct measurement of this effect in high-energy accelerators has been reported.

In this Letter, we report the results of the turn-by-turn measurements of the THz CSR produced by laser slicing at the UVSOR-II electron storage ring operated with low-alpha optics. The results clearly show the existence of the transverse-longitudinal coupling effect.

In laser bunch slicing, a laser pulse of subpicosecond duration interacts with an electron bunch several tens of picoseconds long. An intense laser field modulates the energy of electrons traveling in a periodic magnetic field produced by an undulator. After the interaction, the electrons trace different orbits depending on their energy. This produces differences in orbit length, and hence in longitudinal position. As a result, the energy-modulated electrons escape their original positions and form electron fragments of a subpicosecond duration (see Fig. 1). At the same time, a dip structure is created in the unmodulated electron bunch.

Figure 1 shows a schematic drawing of the laser bunch slicing system at UVSOR-II, which consists of a Ti:sapphire laser system, an undulator, and an IR/THz beam line [12,20]. The laser system provides 2.5 mJ laser pulses with 1 kHz repetition, synchronizing with the rf acceleration of the ring. The rf frequency and the revolution frequency of the ring are 90.1 and 5.6 MHz, respectively. The laser is intense enough to provide energy modulation 10 times larger than the natural energy spread [12].

 

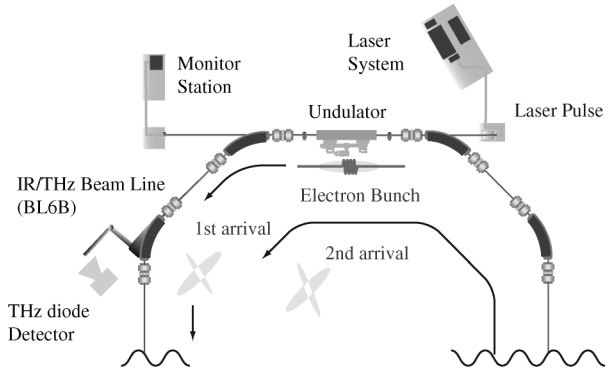


FIG. 1. Schematic drawing of laser bunch slicing system at UVSOR-II.

In this experiment, the ring was operated in single bunch mode, in which only one electron bunch is circulating, with three electron beam optics, the normal optics, and two low-alpha optics with different betatron tunes of 3.53 and 3.68. Since the tune is close to the half and third resonances, we refer to the latter two as low-alpha (1/2) and low-alpha (1/3) optics. The main parameters of the beam optics are shown in Table I. The momentum compaction factor $\alpha_C$ of the low-alpha optics is about one-fifth that of the normal optics.

THz CSR was observed at the IR/THz beam line, whose source point is the second bending magnet from the undulator, using diode detectors with a temporal response of a few hundred picoseconds and a narrow frequency bandwidth. This fast temporal response made it possible to observe THz CSR emitted by the electron bunch turn by turn. Three diode detectors were prepared, which are sensitive to frequency ranges, 11.0–16.6 $cm^{-1}$ (Virginia Diode Instruments, WR2.2ZBD), 7.3–11.0 $cm^{-1}$ (Virginia Diode Instruments, WR3.4ZBD), and 3.7–5.7 $cm^{-1}$ (Millitech, Inc., DXP-06).

For normal optics, although the results are not shown here, the CSR at the first arrival was detected by all three detectors; however, the CSR at the second arrival was observed by only two detectors at the lower frequency ranges, and its intensity was much lower than the first.

TABLE I. Main parameters of a normal and two low-alpha optics.

| | Normal | low $\alpha_C$ (1/2) | low $\alpha_C$ (1/3) |
|---|---|---|---|
| $\alpha_C$ | 0.028 | 0.00615 | 0.00471 |
| $\nu_x$ | 3.75 | 3.53 | 3.68 |
| $\varepsilon_x$ (mm mrad) | 15.6 | 139.2 | 176.8 |
| $\eta_x$ (m)[a] | 0.800 | −1.038 | −1.671 |
| $\eta_x$ (m)[b] | 0.248 | 0.430 | 0.560 |

[a] $\eta_x$ is a dispersion function at the center of the undulator.
[b] $\eta_x$ is a dispersion function at the detector.

After the third arrival, the CSR intensity was below the detection limit.

With the low-alpha (1/2) optics, as shown in Figs. 2(a)–2(c), the CSR is intense at every other turn. In the middle and high-frequency ranges, it is intense at the first and third arrivals. At the low-frequency range, it could be observed up to the 11th arrival. Although the CSR at the third and fifth arrivals is intense, that of the first arrival is weak.

In the low-alpha (1/2) optics, the betatron tune is close to a half integer. Thus, the intermittent CSR emission was expected to be related to the betatron motion. To confirm this, we tried the same experiment with the low-alpha (1/3) optics. Because of the limited beam time, CSR was observed only at the middle frequency range. The result is shown in Fig. 2(d). The CSR is intense at every third arrival, the first and fourth. Weak CSR is also observed at the seventh arrival, despite the absence of CSR at the fifth and sixth.

The evolution of the dip structure may be simulated based on linear beam dynamics theory. In the simulation, the change in the longitudinal position of an electron at the source point $\Delta z$ was expressed by a linear equation,

$$\Delta z = R_{51} x_0 + R_{52} x_0' + R_{56}[\delta_0 + \Delta\delta(z)], \qquad (1)$$

where $x_0$, $x_0'$, and $\delta_0$ are the displacement and slope from the reference orbit in the horizontal plane, and the energy deviation before the interaction, which are Gaussian distributed with root mean square values of the beam size, the angular divergence at the undulator, and the energy spread. Here, we neglect motion in the vertical plane. $\Delta\delta(z)$ is the energy change produced by the laser interaction, whose absolute value is much larger than $\delta_0$. $R_{51}$, $R_{52}$, and $R_{56}$ are the elements of the transport matrix $\mathbf{R}$ [21].

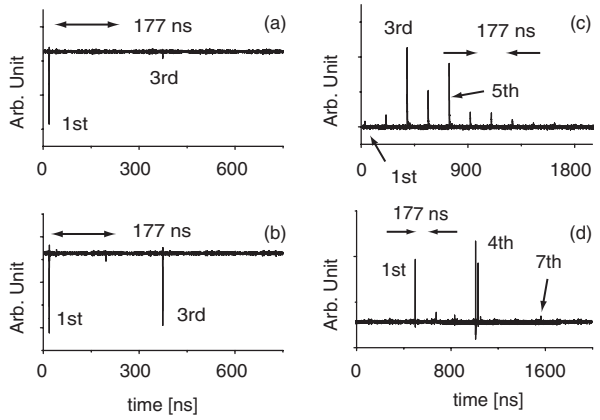


FIG. 2. CSR signals of three diode detectors at the low-alpha optics. Revolution time of the ring is 177 ns. Panels (a)– (c) are with the low-alpha (1/2) optics and a laser pulse FWHM of 460 fs. Sensitivity ranges are (a) 11.0–16.6 $cm^{-1}$, (b) 7.3–11.0 $cm^{-1}$, and (c) 3.7–5.7 $cm^{-1}$. Panel (d) is with low-alpha (1/3) optics and a laser pulse FWHM of 1 ps. Sensitivity range is 7.3—11.0 $cm^{-1}$.

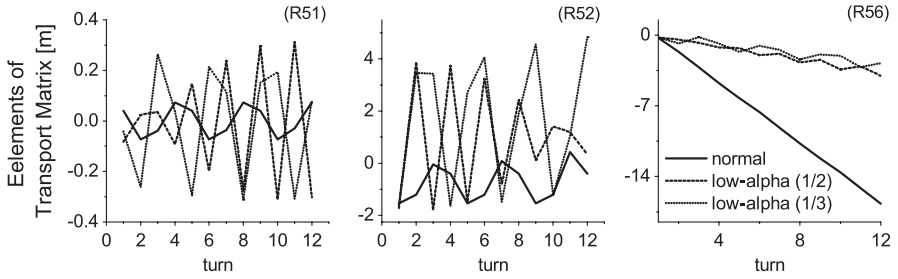


FIG. 3. Development of $R_{51}$, $R_{52}$, and $R_{56}$ elements of transport matrices at each turn at normal and two low-alpha optics.

The transport matrix for the $n$th arrival at the source point can be written as

$$\mathbf{R}^{(n)} = \mathbf{R}_1 \mathbf{R}_C^{(n-1)}, \tag{2}$$

where $\mathbf{R}_C^{(n-1)}$ and $\mathbf{R}_1$ are the matrices for $n-1$ revolutions starting from the undulator and from the undulator point to the source point, respectively. It can be shown that the elements of $\mathbf{R}_C^{(n)}$ are related to the momentum compaction factor $\alpha_C$ as follows,

$$R_{C56}^{(n)} = n\alpha_C L - [\eta_x^* R_{C51}^{(n)} + \eta_{x'}^* R_{C52}^{(n)}], \tag{3}$$

where $L$, $\eta_x^*$, and $\eta_{x'}^*$ are the circumference of the storage ring, the momentum dispersion function, and its slope at the undulator, respectively. The second and third terms in the right-hand side of Eq. (3) appear only when $\eta_x^*$ and $\eta_{x'}^*$ are not zero at the undulator.

Figure 3 shows the turn-by-turn developments of $R_{51}$, $R_{52}$, and $R_{56}$ of the three beam optics. $R_{51}$ and $R_{52}$ oscillate at the betatron tune $\nu$. Oscillation amplitudes are larger at the two low-alpha optics than at the normal optics. The absolute value of $R_{56}$ increases turn by turn with oscillation at the betatron tune. In the case of low-alpha optics, the increase of the absolute value is suppressed and the amplitude of the oscillation increases with increasing $\eta_x^*$ and $\eta_{x'}^*$.

Figure 4 shows numerical estimates of CSR signals, which are obtained from Fourier transform of the simulated longitudinal density structure of the electron bunch. The results are in good agreement with the observational results. In particular, the observed intermittent emissions are well reproduced for both low-alpha optics. Next, we theoretically investigate the origin of such peculiar behaviors of the THz CSR.

To understand the results in detail, the simulated evolution of the dip structure in longitudinal phase space is shown in Fig. 5. It may be helpful to rewrite Eq. (1) for the longitudinal slippage at the undulator after the $n$th turn as

$$\Delta z = R_{C51}^{(n)} x_{0\beta} + R_{C52}^{(n)} x'_{0\beta} + n\alpha_C L[\delta_0 + \Delta\delta(z)]. \tag{4}$$

Here, $x_{0\beta}$ and $x'_{0\beta}$ are the horizontal displacement and its slope due to the betatron oscillation given by

$$x_{0\beta} = x_0 - \eta_x^*[\delta_0 + \Delta\delta(z)], \tag{5}$$

$$x'_{0\beta} = x'_0 - \eta_{x'}^*[\delta_0 + \Delta\delta(z)]. \tag{6}$$

The motion of the laser-modulated electrons may be described as follows. The sudden energy change caused by the laser interaction produces a longitudinal slippage proportional to $\alpha_C$ [third term of the right-hand side of Eq. (4)]. Therefore, fragments of the modulated electron incline gradually according to $\alpha_C$ and a dip is formed. In addition, when the momentum dispersion function at the undulator is not zero, after the laser interaction the electrons start betatron oscillation with large amplitudes around new closed orbits corresponding to their new energy [see Eqs. (5) and (6)]. This betatron oscillation produces another longitudinal slippage through $R_{51}$ and $R_{52}$, which are oscillating with the betatron tunes [first and second terms of the right-hand side of Eq. (4)]. This makes the inclination of the fragments oscillate back and forth as $R_{51}$ and $R_{52}$ are oscillating.

The electrons, which do not interact with the laser pulse [the case of $\Delta\delta(z) = 0$ in Eqs. (4)–(6)], distribute around the closed orbits, and their energy also distributes around the central value. A small energy deviation ($\delta_0$) produces small longitudinal slippage [third term of the right-hand

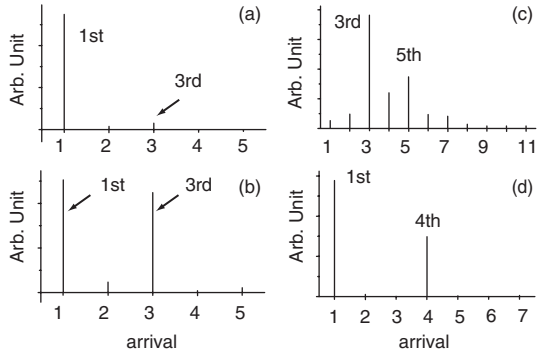


FIG. 4. Numerical estimates of CSR signals at the low-alpha optics. Panels (a)–(c) are with betatron tune 3.53 and a laser pulse FWHM of 460 fs. Sensitivity ranges are (a) 11.0–16.6 $cm^{-1}$, (b) 7.3–11.0 $cm^{-1}$, (c) 3.7–5.7 $cm^{-1}$, and (d) is with betatron tune 3.68 and a laser pulse FWHM of 1 ps. Sensitivity range is 7.3–11.0 $cm^{-1}$.

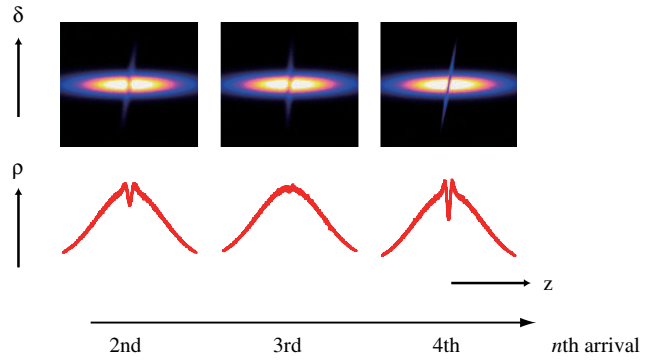


FIG. 5 (color online). An example of evolution of fragments and a dip structure in longitudinal phase space (upper) and its corresponding longitudinal density distribution (lower). The horizontal axis is an arrival order after the revolutions.

side of Eq. (4)]. Thus, the dip inclines gradually in longitudinal phase space, growing wider and shallower and finally disappearing. If $\alpha_C$ is small, the dip structure can last longer. It is interesting that the inclination of the fragments and the dip in longitudinal phase space are not the same when the momentum dispersion at the undulator is not zero (see Fig. 5). In addition, the transverse spread turns into longitudinal spread through $R_{51}$ and $R_{52}$. The dip structure alternately blurs and sharpens as $R_{51}$ and $R_{52}$ are oscillating with the betatron tunes (see Fig. 5). As the combined effect of the mechanisms described above, intermittent CSR was emitted.

We have observed the transverse-longitudinal coupling effect in laser bunch slicing by measuring the THz CSR turn by turn with ultrafast diode detectors. The results were in good agreement with the numerical simulation based on linear beam dynamics theory.

The transverse-longitudinal coupling effect will be of great importance in advanced accelerators based on low-alpha or isochronous optics, such as storage ring light sources dedicated to CSR [7–9] or energy recovery linacs [22]. In such accelerators, the bunch shape depends not only on the longitudinal dynamics but also on the transverse dynamics. In the case of light sources, since the CSR intensity and spectrum would depend on the betatron phase, the source points should be selected carefully. On the other hand, it may be possible to control the interval of intense CSR emission by controlling the betatron tune, which may be useful for time-resolved experiments. This experiment also demonstrated that THz CSR measurement using several diode detectors sensitive to different frequency ranges is a powerful tool for observing evolution of longitudinal microstructures.

We express appreciation for the great help and cooperation of the staff members of the Institute for Molecular Science, K. Ohmori, H. Chiba, J. Yamazaki, K. Hayashi, and E. Nakamura. Fruitful discussion with Y. Kobayashi and K. Ohmi (KEK) is gratefully acknowledged. This study was executed under the support of Grant-in-Aid for Scientific Research (B17360039) and Grant-in-Aid for Young Scientists (B19740150) of JSPS. A part of this study was supported by Quantum Beam Technology program of JST and MEXT.

*miho.shimada@kek.jp

[1] G. L. Carr *et al.*, Nature (London) **420**, 153 (2002).
[2] M. Tonouchi, Nat. Photon. **1**, 97 (2007).
[3] T. Nakazato *et al.*, Phys. Rev. Lett. **63**, 1245 (1989).
[4] M. Abo-Bark *et al.*, Phys. Rev. Lett. **88**, 254801 (2002).
[5] Y. Shoji *et al.*, in *Proceedings of the European Particle Accelerator Conference, Edinburgh, 2006* (EPS-AG, Mulhouse, France, 2006), pp. 163–165.
[6] F. Wang *et al.*, Phys. Rev. Lett. **96**, 064801 (2006).
[7] J. M. Byrd *et al.*, Infrared Phys. Technol. **45**, 325 (2004).
[8] F. Sannibale, A. Marcelli, and P. Innocenzi, J. Synchrotron Radiat. **15**, 655 (2008).
[9] H. Hama *et al.*, New J. Phys. **8**, 292 (2006).
[10] See, for example, J. S. Nodvick and D. S. Saxon, Phys. Rev. **96**, 180 (1954).
[11] R. W. Schoenlein *et al.*, Science **287**, 2237 (2000).
[12] M. Shimada *et al.*, Jpn. J. Appl. Phys. **46**, 7939 (2007).
[13] J. M. Byrd *et al.*, in *Proceedings of the European Particle Accelerator Conference, Lucerne, 2004* (EPS-AG, Mulhouse, France, 2004), pp. 2448–2450.
[14] K. Holldack *et al.*, Phys. Rev. Lett. **96**, 054801 (2006).
[15] V. Schlott *et al.*, in Proceedings of the European Particle Accelerator Conference, 2006, Edinburgh (Ref. [5]), pp. 1229–1231.
[16] S. Bielawski *et al.*, Nature Phys. **4**, 390 (2008).
[17] See, for example, D. Deacon, Phys. Rep. **76**, 349 (1981).
[18] Y. Shoji, Phys. Rev. ST Accel. Beams **7**, 090703 (2004).
[19] X. Huang, Phys. Rev. ST Accel. Beams **10**, 014002 (2007).
[20] S. Kimura *et al.*, Infrared Phys. Technol. **49**, 147 (2006).
[21] See, for example, K. L. Brown, SLAC Report No. 75, 1982.
[22] See, for example, S. Sakanaka *et al.*, in *Proceedings of the European Particle Accelerator Conference, 2008, Genoa* (EPS-AG, Mulhouse, France, 2008), pp. 205–207.